Picojoule threshold, picosecond optical parametric generation in reverse proton-exchanged lithium niobate waveguides

Xiuping Xie, Andrew M. Schober, Carsten Langrock, Rostislav V. Roussev, Jonathan R. Kurz, and Martin M. Fejer

Edward L. Ginzton Laboratory, Stanford University, Stanford, California 94305

Received December 26, 2003; revised manuscript received March 13, 2004; accepted March 16, 2004

We have demonstrated picosecond optical parametric generation in reverse proton-exchanged waveguides in periodically poled lithium niobate with thresholds as low as 200 pJ. Near-transform-limited near-infrared pulses were obtained from cascaded optical parametric generation. For a 1.8-ps (FWHM) pump pulse at 769.6 nm, a saturated internal photon-conversion efficiency of 33% was obtained with 1 nJ of pump energy. The signal-wavelength tuning range was from 1.15 μm to 2.3 μm with a pump wavelength between 770 nm and 789.5 nm. Numerical simulations well predicted the mechanism for the transform-limited pulse generation. These results enable optical parametric generation devices with low threshold and good temporal properties with a simple single-pass setup.

OCIS codes: 190.4410, 190.7110, 190.2620, 320.5390, 320.7080, 070.4550.

1. INTRODUCTION

Low power and compact sources of tunable ultrashort near-infrared and midinfrared pulses are necessary in many applications. Parametric frequency converters that offer very wide tunability and require only a single pump laser have already been studied in detail.[1] Without external resonators, cavity-length stabilization, or seed signals, the single-pass optical parametric generator (OPG) offers inherent simplicity and robustness when compared with other parametric conversion systems, such as the synchronously pumped optical parametric oscillator[2] and the continuum-seeded optical parametric amplifier.[3] However, single-pass pulse OPG has a high threshold, and the temporal properties of the generated pulses depend strongly on the properties of the nonlinear materials.

Recently, ultrashort-pulse OPG systems have been studied extensively to obtain lower threshold, better pulse properties, and higher conversion efficiency. In bulk materials, thresholds as low as 54 nJ with 500-fs pump pulses were reported for periodically poled lithium niobate (PPLN) crystal by utilizing the high nonlinear coefficient in quasi-phase-matched (QPM) devices.[4] Near-transform-limited (temporal and spatial) pulses were obtained with an OPG in specific wavelength configurations.[5–7] Single-pass conversion efficiency of 40% was reached by matching of the group velocities.[8] One current challenge for practical OPG systems is to further lower the OPG threshold to levels attainable directly from laser oscillators while keeping good temporal properties of the pulses. In this paper, we present the results of OPG in reverse-proton-exchanged (RPE) PPLN waveguides.

In waveguides, the trade-off between focusing tightly for high intensities and focusing loosely for avoiding diffraction is eliminated. Thus waveguide geometries can increase the parametric gain by tightly confining the optical fields over long interaction lengths and thereby lower the OPG threshold.[9,10] In the experiments reported here with RPE waveguides in PPLN, a pump pulse with FWHM length of 1.8 ps at 769.6 nm yielded an OPG threshold of 200 pJ. The quasi-phase-matched OPG demonstrated up to 33% saturated photon-conversion efficiency (internal) with 1-nJ pump pulses. The single-pass OPG was tunable from 1.15 μm to 2.3 μm for pump wavelengths between 770 nm and 789.5 nm. Moreover, when the generated outputs are related to a sum-frequency-generation (SFG) process (here called cascaded OPG products), they can be near transform limited, even in the presence of significant group-velocity mismatch (GVM).

2. WAVEGUIDE DEVICE PROPERTIES

The RPE process is based on annealed proton exchange[11] (APE), which has been an important technique for the fabrication of low-loss optical waveguides in $LiNbO_3$. RPE has been used to bury proton-exchanged lithium niobate waveguides and enhance the parametric gain by a factor of >2 over annealed proton exchange waveguides.[12,13] An empirical model that permits accurate calculation of the refractive-index profile of RPE waveguides as a function of the proton-exchange width and depth, and the annealing and reverse-exchange times, has recently been developed.[14] With the higher gain resulting from the improved mode overlap in the more symmetric refractive-index profile, the RPE waveguides have lower OPG thresholds than do the APE waveguides.

For parametric processes in waveguides, because of the phase-matching conditions, only a single waveguide mode interacts at each wavelength. For an optical parametric amplifier, the waveguide is of necessity multimode at the pump wavelength, posing a challenge for the mode

launching. With z cut congruent lithium niobate crystals, only TM modes could satisfy QPM conditions using d_{33}. Moreover, in proton-exchanged lithium niobate, only TM modes are guided. In multimode annealed proton-exchange waveguides, a segmented tapered waveguide is one of the most effective ways to launch the pump beam into the fundamental mode.[15] In RPE waveguides, however, because of the symmetry of the eigenmode in depth, simpler adiabatic tapers also work fairly well. In our typical RPE devices, the width of the channels in the SiO_2 masks for proton exchange (hereafter referred to as the waveguide width) varies from 2 μm in the mode-filter region to 7.5 μm in the nonlinear interaction region. The mode filter and taper lengths are 2 mm and 3 mm, respectively. By launching the pump from the mode-filter side, more than 95% of the power is launched in the TM_{00} mode at the end of the taper with these designs. The remaining power in the higher-order pump modes is too low to reach OPG threshold before the OPG of the TM_{00} mode is in the deep saturation regime and therefore has no effects on our results.

3. NUMERICAL SIMULATIONS

In the experiments, we use uniform QPM gratings and transform-limited pump pulses. Under these conditions, the length of the OPG signal pulse is proportional to the length of the QPM grating and the GVM between the signal and the pump. The signal bandwidth, however, is inversely proportional to the grating length and the GVM between the signal and idler. These properties are similar to those encountered in QPM second-harmonic-generation (SHG) and optical parametric oscillator devices, where combining chirped grating and chirped pump would result in a compressed output pulse.[16,17] The situation turns out to be more complex in OPG, which is seeded with randomly phased vacuum noise.

To evaluate the temporal properties of the OPG outputs, we must solve the set of coupled equations for OPG. Considering also the strong cascaded sum-frequency-generation (SFG) processes in QPM devices and without losing generality, there are four equations. Figure 1 is a diagram for the cascaded processes. The slowly varying envelope approximation is valid in our waveguides; therefore the set of coupled equations is

$$\begin{aligned}
\partial A_s/\partial z + (1/u_s)\partial A_s/\partial t &= i\Gamma_{1s}A_i^*A_p d(z)\exp(i\Delta k_1 z) \\
&\quad + i\Gamma_{2s}A_p^*A_g d(z)\exp(i\Delta k_2 z), \\
\partial A_i/\partial z + (1/u_i)\partial A_i/\partial t &= i\Gamma_{1i}A_s^*A_p d(z)\exp(i\Delta k_1 z), \\
\partial A_p/\partial z + (1/u_p)\partial A_p/\partial t &= i\Gamma_{1p}A_s A_i d(z)\exp(-i\Delta k_1 z) \\
&\quad + i\Gamma_{2p}A_s^*A_g d(z)\exp(i\Delta k_2 z), \\
\partial A_g/\partial z + (1/u_g)\partial A_g/\partial t &= i\Gamma_{2g}A_s A_p d(z)\exp(-i\Delta k_2 z).
\end{aligned} \tag{1}$$

Here we use the subscripts s, i, p, and g for signal, idler, pump, and the SFG between signal and pump. For $j = s, i, p, g$, $A_j(z, t)$ is the envelope of the field, u_j is the group velocity, $\Gamma_{qj} = [(8\pi^2 d_{\text{eff}}^2)/(n_j n_k n_l c\varepsilon_0 \lambda_j^2 A_{\text{eff}}^q)]^{1/2}$ is the parametric gain coefficient (here $n_j n_k n_l$ are the refractive indices of the three waves involved in the $\chi^{(2)}$ processes, λ_j is the vacuum wavelength, d_{eff} is the effective nonlinear coefficient of the QPM material, and A_{eff}^q is the effective area of the nonlinear processes in waveguides, where $q = 1$ is for OPG and $q = 2$ is for SFG), $d(z)$ is the QPM grating function, and $\Delta k_1 = k_s + k_i - k_p$ and $\Delta k_2 = k_s + k_p - k_g$ are the phase mismatch in the OPG and SFG processes. Note that near degeneracy, $\Gamma_{1p}^2 = \eta_{\text{SHG}}$, where in the low conversion limit $\eta_{\text{SHG}} = P_{\text{SHG}}/P_{\text{FH}}^2 L^2$. We assume that pulse durations and device lengths are such that group-velocity dispersion can be neglected.

It is difficult to find any analytical solutions that could give insight into the dynamics of even the conventional OPG processes, so we carried out numerical simulations, using a fast Fourier transform split-step method.[18] The simulation results showed that the temporal properties are determined by the group-velocity mismatches between the interacting waves and that the cascaded processes can lead to a variety of additional phenomena.

In conventional OPG, the time–bandwidth product (TBP) of the signal has a minimum of the order of the ratio between the group index difference $\delta n_{sp}/\delta n_{si}$, where $\delta n_{sp} = |n_s^g - n_p^g|$, $\delta n_{si} = |n_s^g - n_i^g|$, and n_j^g is the group index. From numerical simulation results, it is possible to obtain a transform-limited signal when $|\delta n_{sp}/\delta n_{si}| < 1$, especially if the group index of the pump is between those of the signal and idler.[5–7] For example, in $LiTaO_3$, this condition holds for a pump wavelength of 1.03 μm when the signal wavelength lies between 1.38 μm and 1.63 μm (limiting the idler wavelength to <4 μm).[7] In more general configurations, where the group index of the pump is larger than those for both the signal and idler, the minimum TBP is approached at the high gain limit with a grating length of ~2.5 times the GVM length between the signal and pump. In such cases, transform-limited output could not be easily obtained. In materials like β-barium borate, this had been realized by collinear or noncollinear birefringent phase matching (typically pumped with blue or green lasers) in bulk materials owing to the particular material properties.[8,19] However, in proton-exchanged lithium niobate waveguides, all three waves are collinear and TM polarized and such possibilities are eliminated.

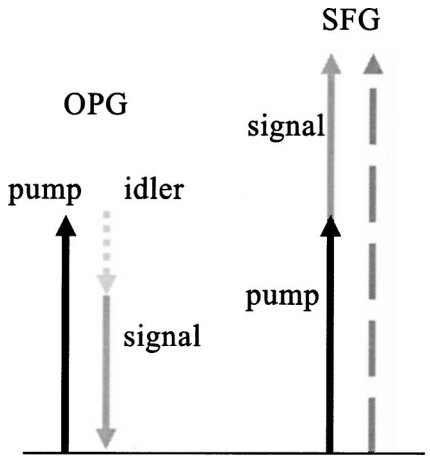

Fig. 1. Diagram of cascaded OPG. The SFG here is between the pump and the signal.

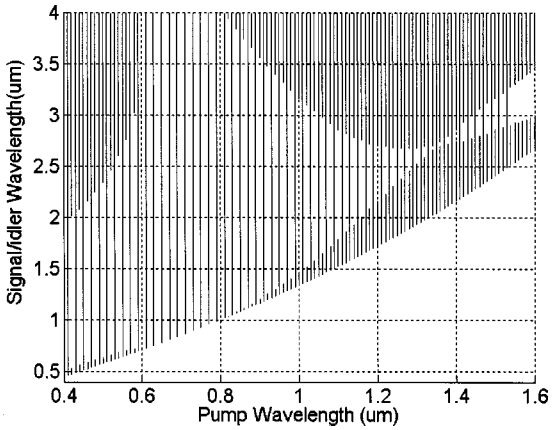

Fig. 2. Transform-limited output ranges permitted by cascaded OPG in bulk $LiNbO_3$, if we limit the idler wavelength to below 4 μm. The double-line shaded region is for the conventional OPG, and the single-line part is the extra region permitted by cascaded OPG.

If the cascaded OPG process is present, because the sum frequency has a higher group index than the pump, the portion of the signal (or idler) from the backconversion of SFG has an apparent effective group velocity slower than the pump. Therefore the group index of the pump is between those of the signal and idler, and the signal output is transform limited. The extended range of transform-limited OPG output in bulk PPLN is shown in Fig. 2. Similar effects would also appear in other nonlinear materials.

In PPLN devices, with a pump wavelength near 780 nm, there are two possible SFG processes satisfying quasi phase matching with a uniform grating period: the second-order ($2K_g = \Delta k$) SFG between idler and pump and the third-order ($3K_g = \Delta k$) SFG between signal and pump. Depending on the duty cycle of the QPM grating, one or both would appear when the pump wavelength is tuned, with the gain coefficient following the formula $G_m(z) = 2\sin(\pi m \times \mathrm{DC})/(\pi m)$. Here m is the order of quasi phase matching, and DC is the duty cycle of the QPM grating. With strong enough SFG gain, not only is the signal transform limited, so also is the visible SFG product. This phenomenon is similar to upconverted parametric generation.[20] The dynamics of the cascaded process is revealed by the numerical simulations: if we fix the grating length and increase the pump power, conventional OPG will reach threshold first, with dips appearing at wavelengths where the SFG QPM condition are satisfied; further increasing the pump power, the cascaded OPG will reach its threshold and grow exponentially faster than the conventional OPG products because of the group-velocity matching. If the QPM grating is long enough, the cascaded OPG products become dominant, and the whole output pulse would be near transform limited. These results were verified in the experiments.

4. EXPERIMENTS AND RESULTS

The pump laser was a mode-locked Ti:sapphire laser generating 1.8-ps (FWHM) transform-limited pulses ~780 nm with 82-MHz repetition rate. A variable attenuator was used to control the peak power of the pulses, while an acoustic optical modulator at 10-kHz repetition rate and 1% duty cycle was used to lower the average power, as a precaution to avoid photorefractive damage (PRD) in the congruent $LiNbO_3$ waveguides. The chips were heated to 120 °C for the same reason. The RPE waveguides had mode filter and taper regions to enable launching of the pump into the fundamental mode of the waveguide, with a waveguide width ~7.5 μm in the nonlinear interaction region, a proton-exchange time of 24.5 h at 171 °C, an annealing time of 22 h at 312 °C, and a reverse-exchange time of 25 h at 300 °C. Several different 0.5-mm-thick PPLN samples fabricated by electric field poling with QPM period from 15 μm to 16.65 μm and grating length from 6 mm to 40 mm were used in the experiment.

The conventional OPG pump throughput and photon-conversion efficiency curves (internal) with 1.8-ps pump pulses at 769.6 nm are shown in Fig. 3. No obvious cascaded OPG was observed in this measurement. The signal wavelength was centered at 1350 nm, with a bandwidth of 10 nm. For this device, the QPM grating period

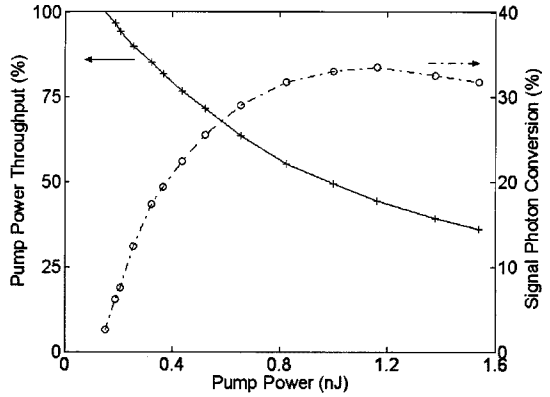

Fig. 3. Pump throughput and the internal signal photon-conversion efficiency in single-pass OPG with a 40-mm-long QPM grating and the absent of cascaded OPG. The pump was 1.8-ps (FWHM) pulse at 769.6 nm, and the signal wavelength was centered at 1350 nm.

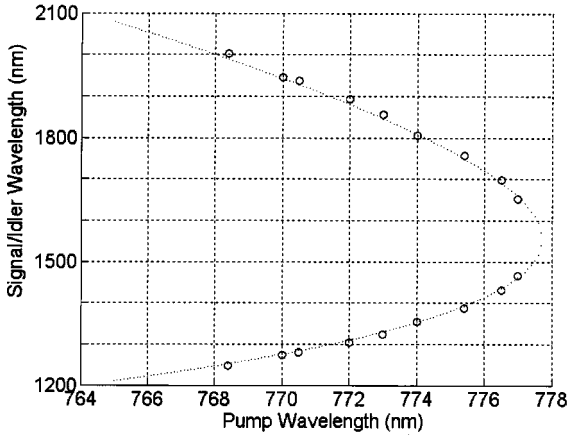

Fig. 4. Pump tuning curve of a RPE PPLN waveguide device (120 °C). The dotted curve is a simulation based on our waveguide dispersion model. The open circles are measurements. The output wavelength ranges from 1245 nm to 2005 nm for pump wavelength between 768.4 nm and 777.5 nm.

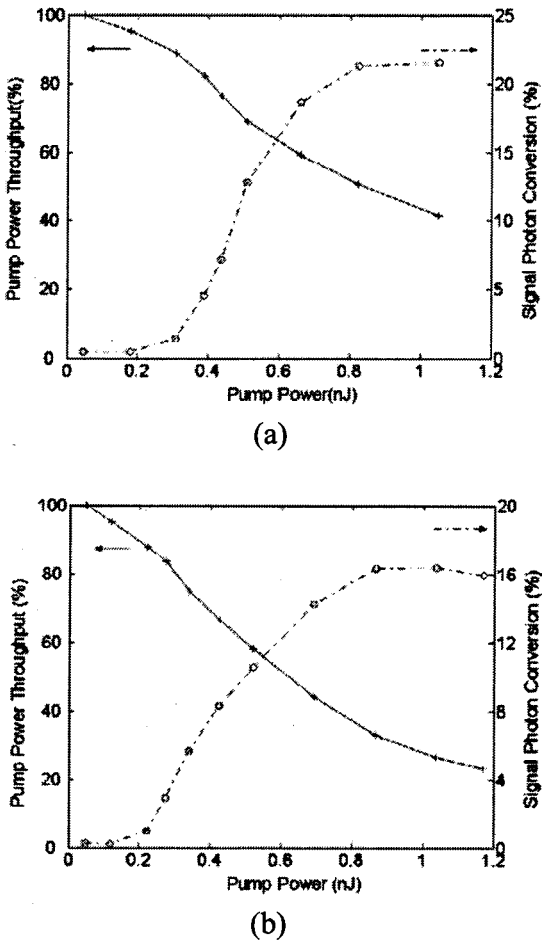

Fig. 5. Internal pump throughput ratio and signal photon-conversion efficiency: (a) for 12-mm-long QPM grating, without cascaded OPG present; (b) for 18-mm-long QPM grating, with cascaded OPG present. Note the decrease in signal photon conversion and the increase in pump depletion in the presence of cascaded OPG.

was 15.75 μm in a 40-mm-long QPM grating, which was ~6 times the signal–pump GVM length. The waveguide width was 7 μm in the interaction regions. The curves in Fig. 3 show an OPG threshold of 200 pJ, matching well with the calculated threshold of 190 pJ, using the measured normalized SHG conversion efficiency (internal) of 90%/(W-cm^2) from similar samples. The maximum saturated internal photon-conversion efficiency was 33%, matching the value of 35% estimated from simulations. The decrease in efficiency after saturation came from the parasitic nonlinear processes including SHG of the pump and the cascaded processes at high pump power.

The typical OPG tuning behavior of the RPE waveguide devices is shown in Fig. 4. The waveguide width was 7.5 μm, and the 18-mm-long grating had a QPM period of 16.25 μm. The theoretical prediction fits the measurements well. In other not-so-well calibrated waveguides, the output wavelengths ranged from 1.15 μm to 2.3 μm for a pump wavelength between 770 nm and 789.5 nm. The tuning range was only limited by the cutoff wavelength of the waveguide, which was estimated to be 2.5 μm for the RPE waveguides in our experiments.

Although the OPG threshold was not affected, the presence of cascaded OPG changed the conversion efficiency as well as the time–bandwidth product dramatically. In the devices with the tuning curve shown in Fig. 4, QPM was satisfied for second-order SFG between the idler and pump, when the pump was ~770 nm and the signal was near 1245 nm. For the same pump power range, the cascaded products were not obvious in the devices with 12-mm-long QPM gratings but became important when the grating length was 18 nm. The internal pump throughput and signal photon-conversion efficiency curves for these two different grating lengths are compared in Fig. 5. Although less signal photon-conversion was recorded in Fig. 5(b), more pump depletion was observed. The emergence of the cascaded OPG decreased the photon conversion into the signal (and idler) because of the sum-frequency output. The thresholds for both cases were near 200 pJ, confirming the results from numerical simulations that the OPG threshold would be stabilized after the grating length was longer than 2.5 times the signal–pump GVM length.

The dynamics of the cascaded OPG process is clearer from the temporal properties, as shown in Fig. 6, which corresponds to the device used for Fig. 5(b). The shape and length of the pulse were measured with a cross correlator based on the two-photon-induced photocurrent using GaAsP photodiodes.[21,22] The reference beam for the cross correlator was a small portion split from the pump before reaching the acousto optical modulator. If we con-

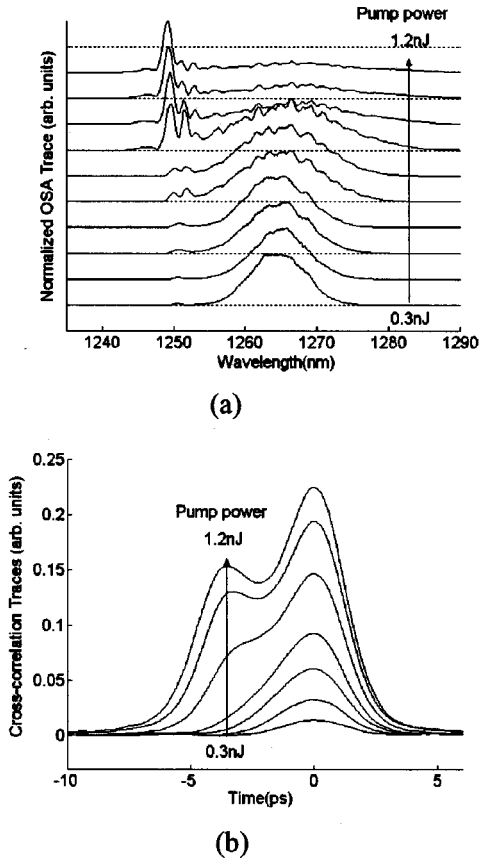

Fig. 6. (a) Optical spectrum analyzer traces; (b) cross-correlation traces for the signal from OPG. Both cover the same pump-power range from 0.3 nJ to 1.2 nJ. Note the shift of spectrum from conventional OPG to cascaded output with increasing pump energy. Cross-correlation traces also show both products.

sider only the cascaded product component, the TBP of the generated signal was 0.51 with a pulse length of 1.9 ps and a bandwidth of 1.4 nm. The conventional OPG product had a TBP of 4.4. Transform-limited TBP for the supposed secant pulse shape is 0.315. By making use of the cascaded process, we have therefore generated a signal with much reduced TBP. The time delay between the two different types of OPG products was 3.6 ps. This means that the cascaded OPG grew up over the last 4 mm of the 18-mm-long grating. Numerical simulations of cascaded OPG predicted that a greater portion of the output would be in the cascaded component with a longer QPM grating length. This was verified by the measurement on the 40-mm gratings (with third-order SFG between the 1420-nm signal and the 769.6-nm pump present), which yielded a cascaded signal with no remaining conventional OPG component observed. The TBP of the square-shaped signal pulse was 0.89, close to the value of 0.886 for a transform-limited square pulse. More studies on the devices with long QPM gratings are in progress.

The OPG threshold can be affected by the propagation loss at the different wavelengths. As we did not have a complete set of loss coefficients, we did not include the loss terms in the coupled equations. While this assumption might cause discrepancy in comparing the experimental and numerical simulations, the effects proved to be small in practice. The two-photon absorption process in waveguides also can affect the results. The high-order quasi-phase-matched SHG of the 780-nm pump generates blue radiation, which is above the two-photon absorption edge. For low-gain devices with SHG conversion efficiency $<10\%/(\text{W-cm}^2)$, it would dominate and deplete the pump before the OPG threshold could be reached. However, for the high-gain RPE waveguide devices, we can ignore it because the OPG gain is exponential, while the SHG gain is quadratic in the grating length. In congruent lithium niobate crystals, PRD was caused by the SFG output at 550-nm or shorter wavelengths. The waveguide devices were slowly damaged by this effect even if they were heated up to 150 °C. Replacing the congruent materials with the MgO-doped lithium niobate crystals in which the PRD threshold is much higher would solve this problem.[23] Pump depletion is another factor that can affect the pulse quality. However, the pulse length and bandwidth are mainly determined before pump depletion since OPG is an exponential process. Minimization of the effects of pump depletion is under investigation.

5. SUMMARY

For picosecond optical parametric generation in RPE waveguides in PPLN, we have demonstrated thresholds as low as 200 pJ. A saturated internal photon-conversion efficiency of 33% was obtained with 1 nJ of pump energy for a 1.8-ps (FWHM) pump pulse at 769.6 nm. The signal-wavelength tuning range was from 1.15 μm to 2.3 μm with a pump wavelength between 770 nm and 789.5 nm. When both OPG and SFG processes were phase matched in the QPM grating, near-transform-limited near-infrared pulses were obtained from cascaded OPG. The mechanism for the transform-limited pulse generation was well predicted by numerical simulations. These results enable low-threshold OPG devices with good temporal properties.

To improve the cascaded OPG process, we are exploring gratings with longitudinally varying duty cycle and designs of phase-modulated QPM gratings[24,25] to control the desired cascade processes. A grating with periodically interlaced OPG and SFG sections is also shown by simulations to generate transform-limited output at the end of the OPG sections. These options will make the sample processing more complex and are still under investigation. After a better knowledge of these approaches is obtained, an integrable tunable device might finally be fabricated and find its applications.

ACKNOWLEDGMENTS

This research was supported by the Defense Advanced Research Projects Agency through the Optoelectronic Materials Center, the U.S. Air Force Office of Scientific Research, through contracts F49620-99-1-0270 and F49620-02-1-0240, and the Stanford Optical Signal Processing Collaboration. We acknowledge the support of Crystal Technology, Inc., New Focus, Inc., and the Stanford Photonics Research Center. X. P. Xie's e-mail address is xpxie@stanford.edu.

REFERENCES

1. W. R. Bosenberg and R. C. Eckardt, eds., special issue on optical parametric devices, J. Opt. Soc. Am. B **12**, 2084–2320 (1995).
2. K. C. Burr, C. L. Tang, M. A. Arbore, and M. M. Fejer, "High-repetition-rate femtosecond optical parametric oscillator based on periodically poled lithium niobate," Appl. Phys. Lett. **70**, 3341–3343 (1997).
3. T. Wilhelm, J. Piel, and E. Riedle, "Sub-20-fs pulses tunable across the visible from a blue-pumped single-pass noncollinear parametric converter," Opt. Lett. **22**, 1494–1496 (1997).
4. A. Galvanauskas, M. A. Arbore, M. M. Fejer, M. E. Fermann, and D. Harter, "Fiber-laser-based femtosecond parametric generator in bulk periodically poled $LiNbO_3$," Opt. Lett. **22**, 105–107 (1997).
5. R. Danielius, A. Piskarskas, A. Stabinis, G. P. Banfi, P. Di Trapani, and R. Righini, "Traveling-wave parametric generation of widely tunable, highly coherent femtosecond light pulses," J. Opt. Soc. Am. B **10**, 2222–2232 (1993).
6. T. Südmeyer, J. Aus. Der. Au, R. Paschotta, U. Keller, P. G. R. Smith, G. W. Ross, and D. C. Hanna, "Novel ultrafast parametric systems: high repetition rate single-pass OPG and fibre-feedback OPO," J. Phys. D **34**, 2433–2439 (2001).
7. T. Südmeyer, F. Brunner, R. Paschotta, T. Usami, H. Ito, M. Nakamura, K. Kitamura, and U. Keller, "Femtosecond optical parametric generation (OPG) in periodically poled stoichiometric $LiTaO_3$ with >1 W average power," *Conference on Lazers and Electro-Optics*, Vol. 73 of OSA Trends in Optics and Photonics Series (Optical Society of America, Washington, D.C., 2002), paper CTuO4.
8. P. Di Trapani, A. Andreoni, C. Solcia, P. Foggi, R. Danielius, A. Dubietis, and A. Piskarskas, "Matching of group velocities in three-wave parametric interaction with femtosecond pulses and application to traveling-wave generators," J. Opt. Soc. Am. B **12**, 2237–2244 (1995).
9. K. Gallo, M. De Micheli, and P. Baldi, "Parametric fluorescence in periodically poled $LiNbO_3$ buried waveguides," Appl. Phys. Lett. **80**, 4492–4494 (2002).
10. M. L. Bortz, M. A. Arbore, and M. M. Fejer, "Quasi-phase-

matched optical parametric amplification and oscillation in periodically-poled $LiNbO_3$ waveguides," Opt. Lett. **20**, 49–51 (1995).
11. M. L. Bortz and M. M. Fejer, "Annealed proton-exchanged $LiNbO_3$ waveguides," Opt. Lett. **16**, 1844–1846 (1991).
12. J. L. Jackel and J. J. Johnson, "Reverse exchange method for burying proton exchanged waveguides," Electron. Lett. **27**, 1360–1361 (1991).
13. K. R. Parameswaran, R. K. Route, J. R. Kurz, R. V. Roussev, M. M. Fejer, and M. Fujimura, "Highly efficient second-harmonic generation in buried waveguides formed by annealed and reverse proton exchange in periodically poled lithium niobate," Opt. Lett. **27**, 179–181 (2002).
14. R. Roussev, X. P. Xie, K. R. Parameswaran, M. M. Fejer, and J. Tian, "Accurate semiempirical model for annealed proton exchanged waveguides in z-cut lithium niobate," *Proceedings of the 16th LEOS Annual Meeting* (IEEE, Piscataway, N.J., 2003), paper TuS4.
15. M. H. Chou, M. A. Arbore, and M. M. Fejer, "Adiabatically tapered periodic segmentation of channel waveguides for mode-size transformation and fundamental mode excitation," Opt. Lett. **21**, 794–796 (1996).
16. G. Imeshev, M. A. Arbore, M. M. Fejer, A. Galvanauskas, M. G. Fermann, and D. Harter, "Ultrashort pulse second-harmonic generation with longitudinally nonuniform quasi-phase-matching gratings: pulse compression and shaping," J. Opt. Soc. Am. B **17**, 304–318 (2000).
17. T. Beddard, M. Ebrahimzadeh, T. D. Reid, and W. Sibbett, "Five-optical-cycle pulse generation in the mid infrared from an optical parametric oscillator based on periodically poled lithium niobate," Opt. Lett. **25**, 1052–1054 (2000).
18. G. P. Agrawal, "Split-step Fourier method," in *Nonlinear Fiber Optics*, 3rd ed. (Academic, New York, 2001), pp. 51–55.
19. A. V. Smith, "Group-velocity-matched three-wave mixing in birefringent crystals," Opt. Lett. **26**, 719–721 (2001).
20. R. Danielius, A. Piskarskas, P. Di Trapani, A. Andreoni, C. Solcia, and P. Foggi, "Visible pulses of 100 fs and 100 mJ from an upconverted parametric generator," Appl. Opt. **35**, 5336–5339 (1996).
21. J. K. Ranka, L. Gaeta, A. Baltuska, M. S. Pshenichnikov, and D. A. Wiersma, "Autocorrelation measurement of 6-fs pulses based on the two-photon-induced photocurrent in a GaAsP photodiode," Opt. Lett. **22**, 1344–1346 (1997).
22. W. Schade, D. L. Osborn, J. Preusser, and S. R. Leone, "Two-color cross-correlation of fs-laser pulses by two-photon induced photoconductivity for near and far field optical measurements," Opt. Commun. **150**, 27–32 (1998).
23. Y. Furukawa, K. Kitamura, S. Takekawa, A. Miyamoto, M. Terao, and N. Suda, "Photorefraction in $LiNbO_3$ as a function of [Li]/[Nb] and MgO concentrations," Appl. Phys. Lett. **77**, 2494–2496 (2000).
24. M. H. Chou, K. R. Parameswaran, and M. M. Fejer, "Multiple-channel wavelength conversion by use of engineered quasi-phase-matching structures in $LiNbO_3$ waveguides," Opt. Lett. **24**, 1157–1159 (1999).
25. M. Asobe, O. Tadanaga, H. Miyazawa, Y. Nishida, and H. Suzuki, "Multiple quasi-phase-matched $LiNbO_3$ wavelength converter with a continuously phase-modulated domain structure," Opt. Lett. **28**, 558–560 (2003).